JOURNAL OF SOLID STATE CHEMISTRY **126,** 127–134 (1996)
ARTICLE NO. 0320

Structure Determination of Two Polymorphic Phases of $La(NO_3)_3 \cdot 4H_2O$ from X-Ray Powder Diffraction

A.-E. Gobichon, M. Louër, J. P. Auffrédic, and D. Louër

Laboratoire de Cristallochimie, CSIM (URA CNRS 1495), Université de Rennes, Avenue du Général Leclerc, 35042 Rennes Cedex, France

Received March 29, 1996; accepted July 10, 1996

The structure of two polymorphic phases of lanthanum nitrate tetrahydrate, prepared from the thermal decomposition of the hexahydrate compound, have been determined from conventional monochromatic X-ray powder diffraction data. The α phase has a monoclinic unit cell with the parameters $a = 6.7778(9)$ Å, $b = 11.3673(1)$ Å, $c = 6.5843(1)$ Å, $\beta = 90.644(5)°$, space group $P2_1/m$. The β phase is orthorhombic with the unit cell parameters $a = 11.834(1)$ Å, $b = 12.973(1)$ Å, $c = 13.531(1)$ Å, space group *Pbca*. For the α phase, atomic coordinates were found by interpretation of one Patterson and three difference Fourier maps, while for the β phase the starting model was the crystal structure of the related cerium compound. The structure models were refined by the Rietveld method. The structures consist of infinite chains along [001], built from 11-fold coordinated and 10-fold coordinated La atoms in the α and β phases, respectively, and linked by bridging nitrate groups. The cohesion of the structures is ensured by hydrogen bonds.

INTRODUCTION

As reported by Leskelä and Niinistö (1), limited structural information is available for low hydrates of rare earth nitrates. This is due to metastability problems and difficulty in isolating single phases. However, it has been shown from the structure determination of lanthanum nitrate hexahydrate, $La(NO_3)_3 \cdot 6H_2O$, that La atoms have 11-fold coordination, which is not common in purely inorganic lanthanum compounds (2). Although the thermal decomposition of this hexahydrate has been studied extensively (3, 4), we have recently reconsidered its behavior by using temperature-dependent X-ray powder diffraction and shown that two polymorphic varieties of lanthanum nitrate tetrahydrate can be synthesized (5). These two phases, α- and β-$La(NO_3)_3 \cdot 4H_2O$, can be obtained in a powder form by changing the water-vapor pressure during the thermal decomposition of the hexahydrated phase. Then, it is of interest to know the crystal structure of these phases and, consequently, the coordination of La atoms. These thermal decomposition products are powders and, although structure determination from powder diffraction has progressed significantly in the past ten years, only a few studies of such compounds have been reported (6, 7). Indeed, the loss of resolution in the diffraction pattern of these compounds resulting from diffraction-line broadening, often anisotropic, which arises from small crystallite size and lattice microdistortion restricts the structure investigation. However, there is a need to know the crystal structures of the successive intermediate solids obtained from the decomposition of a precursor into a finely divided oxide, frequently used in microstructure-dependent technological applications, e.g., catalysis. The present study deals with an X-ray powder diffraction investigation of the crystal structure of the two varieties of lanthanum nitrate tetrahydrate.

EXPERIMENTAL

Material Preparation

The two varieties α- and β-$La(NO_3)_3 \cdot 4H_2O$ were prepared, at 318 K, from the dehydration of $La(NO_3)_3 \cdot 6H_2O$ under water-vapor pressures of 10 and 1.9 Torr, respectively. Their domains of thermodynamical stability have been defined elsewhere (5). In these preparations, the water-vapor pressure was generated from a flask containing a sulfuric acid solution maintained at a constant temperature. The water-vapor pressure was calculated from data reported by Boll (8). The loss of two water molecules from the precursor was confirmed from TG measurements (5).

X-Ray Powder Diffraction

X-ray powder diffraction data were collected at room temperature with a D500 Siemens powder diffractometer equipped with an incident-beam monochromator ($CuK\alpha_1$ radiation), the resolution and precision characteristics of which have been reported elsewhere (9, 10). Patterns were scanned with a step length of $0.02°(2\theta)$ over the angular ranges $12°–107°(2\theta)$ with a counting time of 56 sec step^{-1} for α-$La(NO_3)_3 \cdot 4H_2O$ and $10°–80°(2\theta)$ with a counting

0022-4596/96 $18.00

TABLE 1
Details of the Rietveld Refinement for α- and β-$La(NO_3)_3 \cdot 4H_2O$

Formula	α-$La(NO_3)_3 \cdot 4H_2O$	β-$La(NO_3)_3 \cdot 4H_2O$
Space group	$P2_1/m$	$Pbca$
Z	2	8
Wavelength (Å)	1.540598	1.540598
2θ range (°)	12–107	10–80
Step increment (°2θ)	0.02	0.02
No. of reflections	640	634
No. of structural parameters	33	57
No. of profile parameters	16	14
No. of atoms	11	17
R_F	0.050	0.061
R_B	0.073	0.103
R_P	0.058	0.097
R_{WP}	0.077	0.124

time of 46 sec step^{-1} for β-$La(NO_3)_3 \cdot 4H_2O$. No reliable intensities were observed at higher angles, a consequence of diffraction-line broadening. The samples were deposited in an enclosed sample holder designed to keep them in a stream of nitrogen to prevent hydration. At the end of data collection, the stability of the samples, as well as of the X-ray source, was checked by measuring the first few lines in the patterns again. The peak positions were obtained with the pattern decomposition program PROFILE from Socabim, available in the software package DIFFRAC-AT supplied by Siemens. For the structure analysis, integrated intensities were extracted by means of the iterative pattern decomposition algorithm incorporated in the Rietveld program FULLPROF (11). The structure solutions were obtained from the program SHELX (12, 13). All calculations were performed on a PC-486 computer (14).

TABLE 2
Atomic Coordinates and Thermal Parameters with Their Standard Deviations for α-$La(NO_3)_3 \cdot 4H_2O$

Atom	x	y	z	B_{iso}(Å^2)
La	0.3690(2)	0.25	0.2008(3)	0.63(6)
N1	0.493(3)	0.25	0.746(3)	1.01(4)
O11	0.474(1)	0.154(1)	−0.148(2)	1.45(5)
O12	0.514(2)	0.25	0.568(2)	1.45(5)
N2	0.199(2)	−0.003(1)	0.282(2)	1.01(4)
O21	0.206(1)	0.036(1)	0.101(2)	1.45(5)
O22	0.105(2)	−0.095(1)	0.326(2)	1.45(5)
O23	0.278(1)	0.043(1)	0.437(2)	1.45(5)
OW1	0.079(2)	0.25	−0.077(2)	0.64(1)
OW2	0.021(2)	0.25	0.370(2)	0.64(1)
OW3	0.688(1)	0.1024(8)	0.231(1)	0.64(1)

TABLE 3
Atomic Coordinates and Thermal Parameters with Their Standard Deviations for β-$La(NO_3)_3 \cdot 4H_2O$

Atom	x	y	z	B_{iso}(Å^2)
La	0.1725(3)	0.2185(2)	0.1226(3)	0.32(1)
N1	0.036(4)	0.016(4)	0.142(4)	2.87(8)
O11	−0.023(3)	−0.057(2)	0.151(3)	2.45(7)
O12	0.133(3)	0.026(2)	0.178(2)	0.29(4)
O13	−0.003(3)	0.095(2)	0.096(2)	0.29(4)
N2	0.126(3)	0.195(3)	0.368(5)	2.87(8)
O21	0.222(3)	0.164(2)	0.355(3)	2.45(7)
O22	0.082(3)	0.226(3)	0.448(3)	0.29(4)
O23	0.063(3)	0.211(3)	0.291(3)	0.29(4)
N3	0.002(4)	0.406(3)	0.113(4)	2.87(8)
O31	−0.063(3)	0.476(3)	0.104(3)	2.45(7)
O32	0.110(2)	0.414(2)	0.118(3)	0.29(4)
O33	−0.029(2)	0.311(2)	0.123(3)	0.29(4)
OW1	0.218(2)	0.100(3)	−0.031(2)	0.31(4)
OW2	0.358(2)	0.124(2)	0.161(2)	0.31(4)
OW3	0.329(3)	0.318(2)	0.030(2)	0.31(4)
OW4	0.279(2)	0.342(2)	0.249(2)	0.31(4)

TABLE 4
Selected Bond Distances (Å) and Angles (°) for α-$La(NO_3)_3 \cdot 4H_2O$

Bond distances	
La–O11,O11^{i}	2.65(1)
La–O12	2.60(2)
La–O21,O21^{i}	2.75(1)
La–O23,O23^{i}	2.89(1)
La–OW1	2.67(1)
La–OW2	2.62(1)
La–OW3,OW3^{i}	2.74(1)
N1–O11^{ii},O11^{iii}	1.29(2)
N1–O12	1.18(2)
N2–O21	1.27(2)
N2–O22	1.25(2)
N2–O23	1.26(2)
Angles	
O11^{ii}–N1–O11^{iii}	114(2)
O11^{ii}–N1–O12 (×2)	123(3)
O21–N2–O22	122(3)
O21–N2–O23	125(3)
O22–N2–O23	112(2)
Possible hydrogen bonds	
OW1^{iv}–O22^{v},O22^{vi}	2.69(1)
OW2–O22^{vii},O22^{viii}	2.80(1)

Note. Symmetry code: (i) $x, \frac{1}{2} - y, z$; (ii) $x, y, 1 + z$; (iii) $x, \frac{1}{2} - y, 1 + z$; (iv) $1 + x, y, z$; (v) $1 - x, \frac{1}{2} + y, -z$; (vi) $1 - x, -y, -z$; (vii) $-x, \frac{1}{2} + y, 1 - z$; (viii) $-x, -y, 1 - z$.

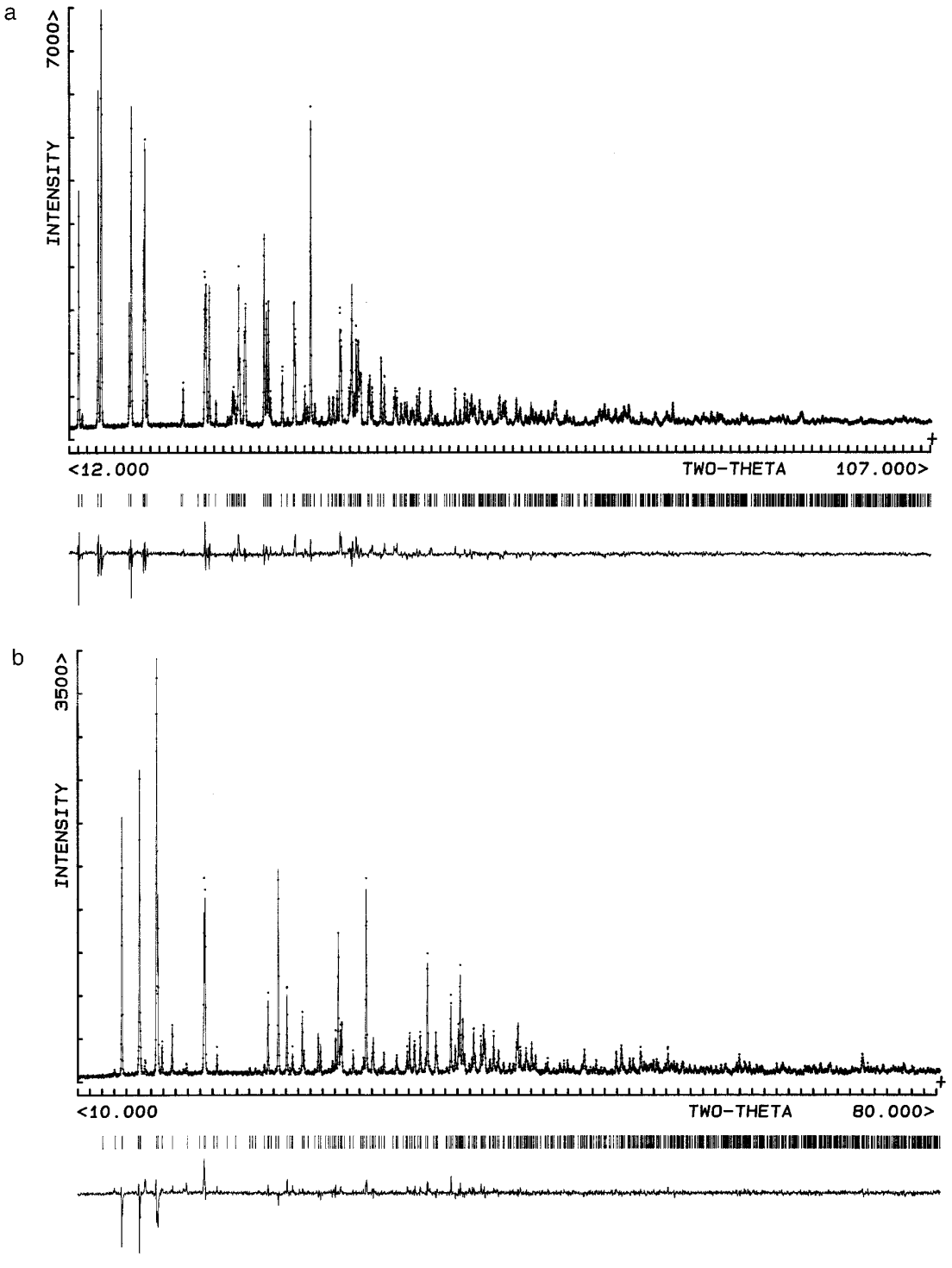

FIG. 1. The final Rietveld plot for α-$La(NO_3)_3 \cdot 4H_2O$ (a) and β-$La(NO_3)_3 \cdot 4H_2O$ (b). The upper traces show the observed data as dots, while the calculated patterns are shown by solid lines. The vertical markers show positions calculated for Bragg reflections. The lower traces are the difference between observed and calculated patterns.

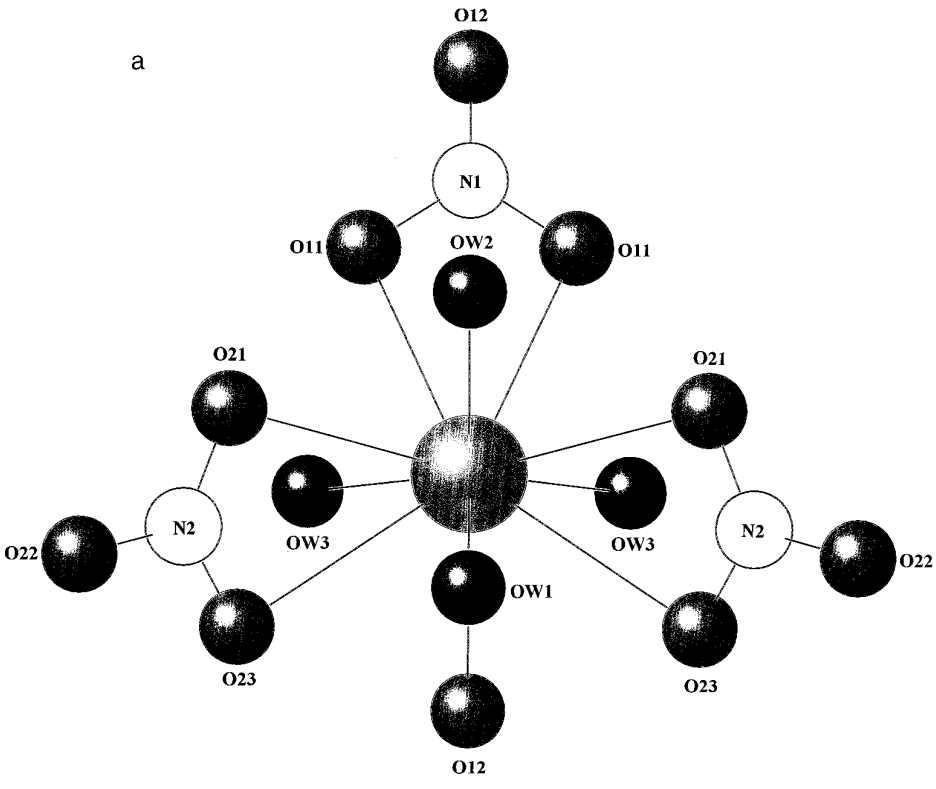

FIG. 2. Lanthanum polyhedra in α-$La(NO_3)_3 \cdot 4H_2O$ (a), β-$La(NO_3)_3 \cdot 4H_2O$ (b), and $La(NO_3)_3 \cdot 6H_2O$ (c).

STRUCTURE DETERMINATION

Indexing of the Powder Diffraction Patterns

Indexing of the powder diffraction patterns was performed by the successive dichotomy method (15) with the program DICVOL91 (16). The first 20 lines were used with an absolute angular error of 0.03°(2θ). The following results were obtained:

(i) α-$La(NO_3)_3 \cdot 4H_2O$. Monoclinic unit cell characterized by the figures of merit $M_{20} = 40$ and $F_{20} = 71(0.0097,29)$. The solution was used for reviewing the powder diffraction data available (50 lines) by means of the computer program NBS*AIDS83 (17). From this evaluation of data quality, the least-squares refined cell dimensions were found to be $a = 6.7778(9)$ Å, $b = 11.3673(1)$ Å, $c = 6.5843(1)$ Å, and $\beta = 90.644(5)°$, with $V = 507.26(1)$ Å^3. The systematic absences were found consistent with the space groups $P2_1$ and $P2_1/m$. The structure solution described below was solved in the space group $P2_1/m$. The final figures of merit, taking into account the space group constraints, are $M_{20} = 31$ and $F_{30} = 64(0.011,42)$. The indexing solution was used to interrogate the NIST CDF database (18) and no chemically related isostructural material of known structure was found.

(ii) β-$La(NO_3)_3 \cdot 4H_2O$. Orthorhombic unit cell characterized by the figures of merit $M_{20} = 39$ and $F_{20} = 77(0.0036,73)$. The solution was used for reviewing the powder diffraction data available (53 lines) by means of the computer program NBS*AIDS83 (17). From this evaluation of data quality, the refined cell dimensions were found to be $a = 11.834(1)$ Å, $b = 12.973(1)$ Å, and $c = 13.531(1)$ Å, with $V = 2077.3(2)$ Å^3. The systematic absences were found consistent with the space group *Pbca*. The final figures of merit, taking into account the space group constraints, were $M_{20} = 60$ and $F_{30} = 85(0.0048,74)$. The indexing solution was also used to interrogate the NIST-CDF database (18), from which the existence of an isostructural relationship with the chemically related material $Ce(NO_3)_3 \cdot 4H_2O$ was revealed.

The powder diffraction data for both phases have been deposited with the ICDD (19).

Structure Determinations and Refinements

(i) α-$La(NO_3)_3 \cdot 4H_2O$. The crystal structure was solved *ab initio* from the powder diffraction data. A Patterson map was calculated from 640 extracted $|F_{obs}|$ values, from which the heavy-atom position was derived. The remaining atoms were located from the calculation of three successive Fourier maps. The approximate atomic coordinates were used as a starting structural model in the Riet-

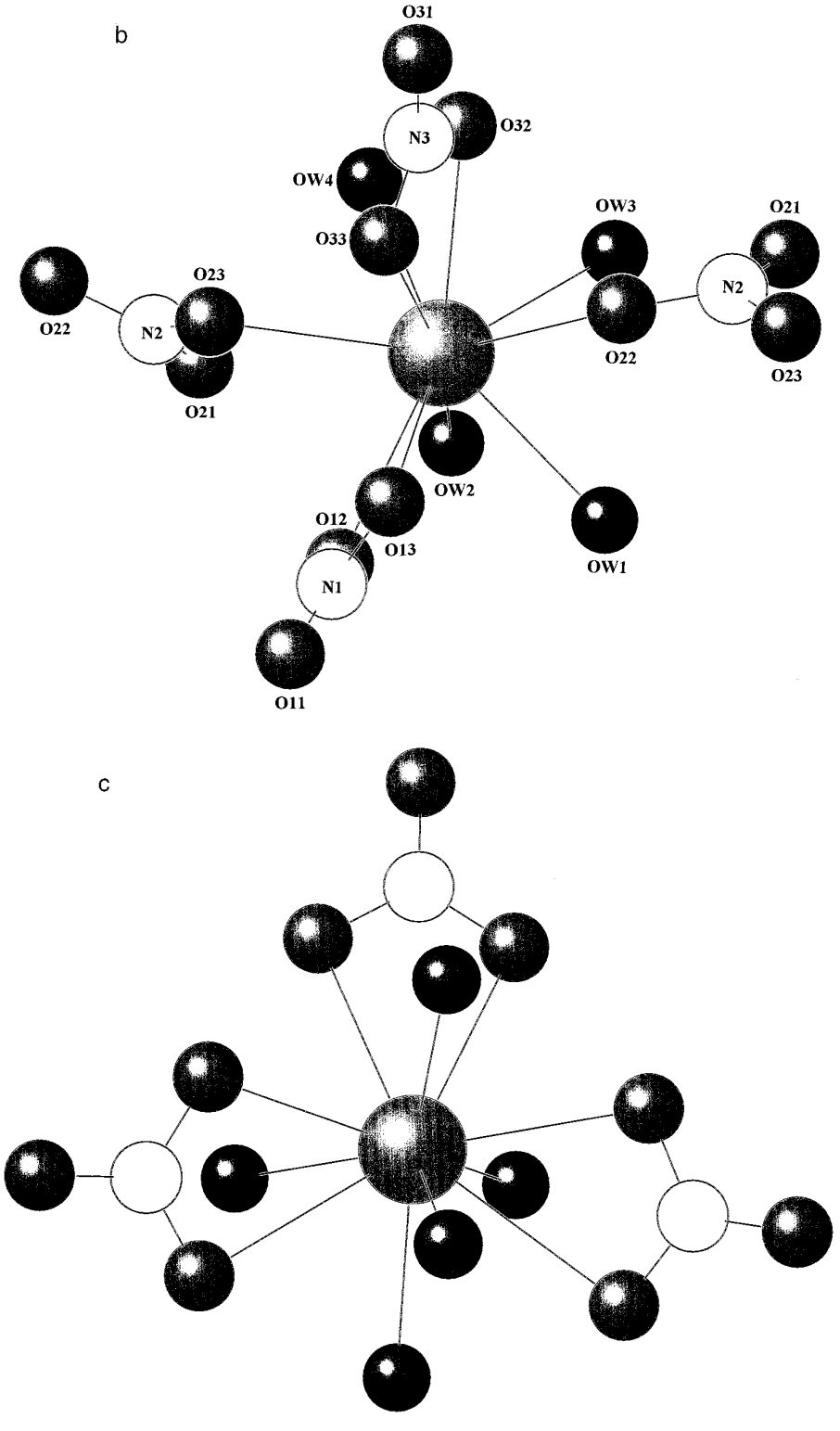

FIG. 2—*Continued*

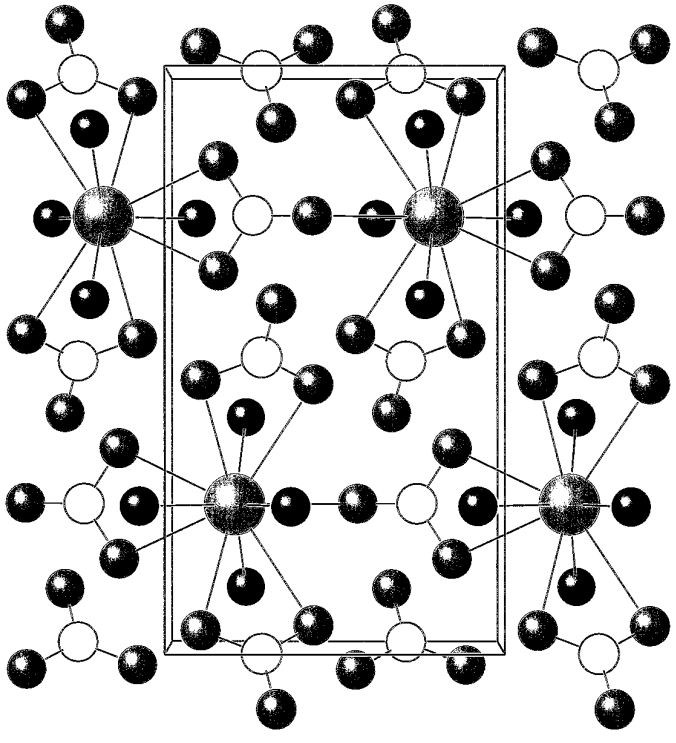

FIG. 3. Perspective view along the *a* axis of the crystal structure of α-$La(NO_3)_3 \cdot 4H_2O$ (*b* vertical and *c* horizontal).

veld refinement. A pseudo-Voigt function was selected to describe individual line profiles with an angular variation of the mixing parameter η. Integrated intensities were distributed over five FWHMs on each side of a diffraction line. The usual quadratic form in tan θ was used to describe the angular dependence of peak widths. The final refinement involved the following parameters: 1 scale factor; 32 structural parameters, including 28 atomic parameters and 4 isotropic thermal factors; 1 zero-point and 4 cell parameters, 3 peak half-width parameters, 1 asymmetry factor, 2 parameters to define the θ-dependent profile shape function, and 5 coefficients to describe the functional dependence of the background. Crystallographic data and details of the Rietveld refinement are given in Table 1. The Rietveld plot in Fig. 1a shows the best agreement obtained between calculated and observed profiles. This fit corresponds to satisfactory crystal-structure model indicators ($R_F = 5.0\%$ and $R_B = 7.3\%$) and profile factors ($R_P = 5.8\%$ and $R_{WP} = 7.7\%$). Final atomic position parameters are given in Table 2.

(ii) *β-$La(NO_3)_3 \cdot 4H_2O$.* Since this phase is isostructural with the chemically related Ce compound, the atomic coordinates of $Ce(NO_3)_3 \cdot 4H_2O$ (20) were used as starting model in the Rietveld refinement. The parameters refined included: 1 scale factor, 56 structural parameters (51 atomic coordinates and 5 isotropic thermal parameters), and 14 instrumental parameters. Crystallographic data and details

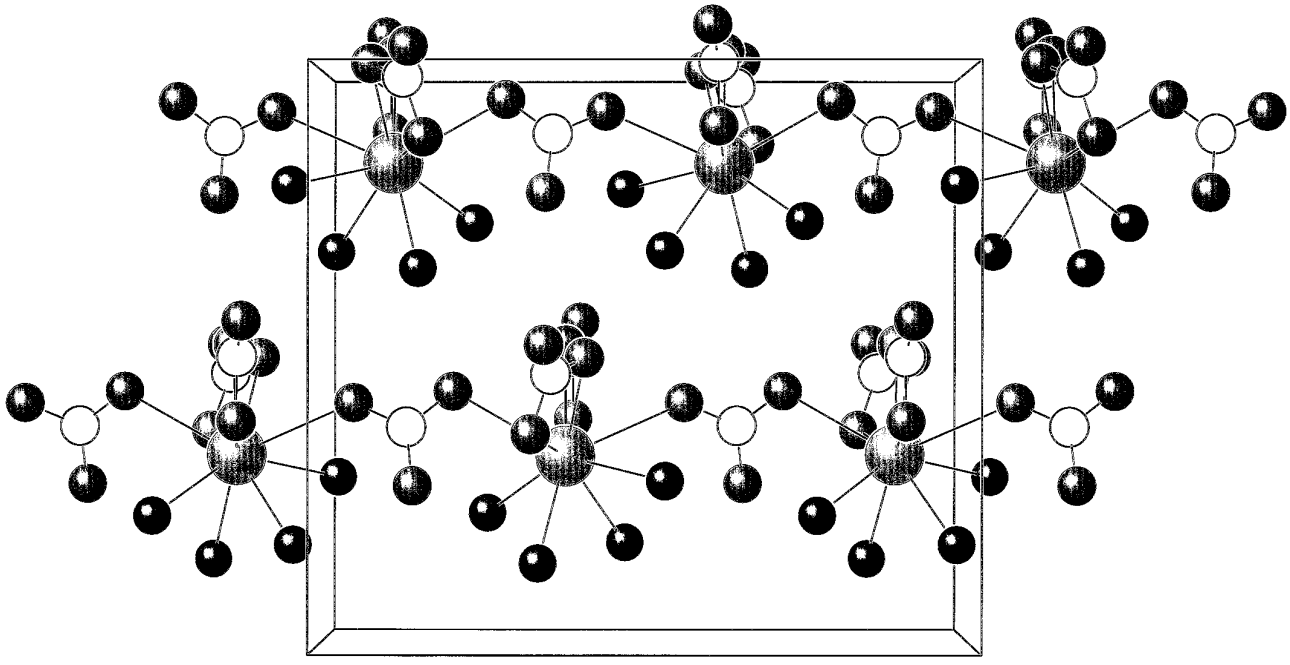

FIG. 4. Perspective view along the *b* axis of the crystal structure of β-$La(NO_3)_3 \cdot 4H_2O$ (*a* vertical and *c* horizontal). Only half the lanthanum polyhedra (related to La at $y = 0.22$) are shown, the other polyhedra ($y = 0.78$) are omitted for clarity.

of the Rietveld refinement are given in Table 1. Although the number of varied parameters is high with respect to the medium quality of the data, the refinement converged to satisfactory crystal-structure model and profile indicators (R_F = 6.1%, R_B = 10.3%, R_P = 9.7%, R_{WP} = 12.4%) and acceptable bond lengths and angles. The Rietveld plot in Fig. 1b shows the best agreement obtained between calculated and observed profiles. Final atomic position parameters are given in Table 3.

DESCRIPTION AND DISCUSSION OF THE STRUCTURES

The structures of the two polymorphic phases consist of infinite chains along the [001] direction, in which the lanthanum polyhedra are connected by means of nitrate groups. However, the two structures present significantly different structural features, resulting essentially from a difference in the coordination of lanthanum (Fig. 2).

(i) *α-$La(NO_3)_3 \cdot 4H_2O$.* The lanthanum atom is surrounded by seven oxygen atoms belonging to three bidentate and one monodentate nitrate groups. Four water molecules complete the La coordination to 11 (Fig. 2a). The La–O(NO_3) and La–O(H_2O) distances are in the range 2.60–2.89 Å and 2.62–2.74 Å (Table 4), respectively, and agree well with values reported for the 11-fold coordinated hexahydrate complex, namely 2.617–2.875 Å and 2.526–2.668 Å (2). The monodentate nitrate (N1) also acts as a bidentate-bridging ligand with the neighboring La polyhedron, giving rise to the formation of chains along the *c* axis (Fig. 3). The cohesion of the structure is ensured by hydrogen bonds between the terminal O atoms (O22) of the bidentate nitrate groups and water molecules in neighboring chains (Table 4). The three bidentate and the monodentate nitrate groups belong, respectively, to the classes I_{2b} and II_4 proposed by Leclaire (21). The monodentate (through O12) and bidentate (through O11 × 2) functions of the nitrate (N1) involve different N1–O distances and angles. The N1–O12 distance (1.18 Å) is shorter than that for the N1–O11 distance (1.29 Å) and the O11–N1–O11 angle is smaller (114°) than the two others (123°).

(ii) *β-$La(NO_3)_3 \cdot 4H_2O$.* The lanthanum atom is surrounded by 10 oxygen atoms. Six are from two bidentate and two monodentate nitrate groups, and four are from water molecules (Fig. 2b). The La–O(NO_3) and La–O(H_2O) distances are in the range 2.62–2.69 Å and 2.57–2.66 Å (Table 5), respectively. The monodentate nitrates act as bridging ligands between adjacent polyhedra, from which arise the chains along the *c* axis (Fig. 4). Again the cohesion of the structure is ensured by hydrogen bonds between water molecules, all located on one side of the La polyhedra, and the terminal O atoms of nitrate groups (Table 5). The bidentate nitrate groups belong to the Leclaire class I_{2b}. In each nitrate group, the distances from the N atom to the noncoordinated O atom are significantly shorter (1.19 Å) than the other distances (mean value: 1.28 Å). The displacement parameters of these terminal O atoms are greater than those found for the coordinated O atoms. The O–N–O angles between the two coordinated O atoms are smaller (mean value: 113.5°) than the O–N–O angles involving a terminal O atom (mean value: 123.5°). The monodentate nitrate groups are of class II_5 and, for the same reason, the distance between the noncoordinated O atom and the N atom is shorter (1.22 Å) than the others (mean value: 1.28 Å).

From the structure determination of the two varieties of lanthanum nitrate tetrahydrate an observation deserves to be discussed. In the hexahydrate compound, the 11-fold coordinated lanthanum polyhedra (Fig. 2c) are independent, all nitrate groups are bidentate, and the environment contains five additional water molecules. The sixth water molecule in the structure is ''free'' and ensures the cohesion of the structure through hydrogen bonds. From the two structures solved in this study, it can be noted that the dehydration process of the triclinic hexahydrate, with the loss of two water molecules, can be logically described.

TABLE 5
Selected Bond Distances (Å) and Angles (°) for β-$La(NO_3)_3 \cdot 4H_2O$

Bond distances			
La–O12	2.65(3)	N1–O11	1.19(6)
La–O13	2.65(3)	N1–O12	1.25(6)
La–O22[i]	2.69(4)	N1–O13	1.30(6)
La–O23	2.62(4)	N2–O21	1.22(5)
La–O32	2.65(3)	N2–O22	1.26(8)
La–O33	2.67(3)	N2–O23	1.30(7)
La–OW1	2.65(3)	N3–O31	1.19(6)
La–OW2	2.57(3)	N3–O32	1.29(5)
La–OW3	2.58(3)	N3–O33	1.29(7)
La–OW4	2.66(3)		

Angles	
O11–N1–O12	126(8)
O11–N1–O13	118(7)
O12–N1–O13	116(7)
O21–N2–O22	128(9)
O21–N2–O23	118(8)
O22–N2–O23	114(8)
O31–N3–O32	126(8)
O31–N3–O33	123(8)
O32–N3–O33	111(5)

Possible hydrogen bonds	
OW1–O11[ii]	2.87(1)
OW3–O21[i]	2.69(1)
OW4–O21	2.79(1)
OW1–O31[iii]	2.93(1)

Note. Symmetry code (i) $x, \frac{1}{2} - y, -\frac{1}{2} + z$; (ii) $-x, -y, -z$; (iii) $\frac{1}{2} + x, \frac{1}{2} - y, -z$.

Indeed, the free molecule could easily be removed, but a collapse of the structure framework should be considered to form a hypothetical pentahydrate. Moreover, if an additional water molecule from the La polyhedron leaves the structure, a simple rearrangement of the framework is possible by a condensation of individual polyhedra through bridging nitrate groups to form chains. It is this second alternative which explains the relationship between the hexa- and the α- and β-tetrahydrates.

To conclude, this powder diffraction study has clearly shown that two polymorphs of $La(NO_3)_3 \cdot 4H_2O$ are obtained for different water-vapor pressures. The two structures are built from chains formed with La polyhedra, but their coordination differs in the two phases, i.e., 11- and 10-fold coordination. It has been shown that the structures of the α phase and the hexahydrate are directly related and that the peculiarity of the 11-fold coordination of lanthanum is conserved in both phases. The identification of two tetrahydrated polymorphs with significant structural differences is responsible for the two different thermal decomposition schemes reported elsewhere (5).

REFERENCES

1. M. Leskelä and L. Niinistö, "Handbook of the Physics and Chemistry of the Rare Earths" (K. A. Gscheidner Jr. and L. Eyring, Eds.), Vol. 8, p. 302. North-Holland, Amsterdam, 1986.
2. B. Eriksson, L.-O. Larsson, L. Niinistö, and J. Valkonen, *Inorg. Chem.* **19,** 1207 (1980).
3. W.-W. Wendlandt, *Anal. Chim. Acta* **15,** 435 (1956).
4. M. Karppinen, P. Kyläkoski, L. Niinistö, and C. Rodellas, *J. Thermal Anal.* **35,** 347 (1989).
5. A.-E. Gobichon, J. P. Auffrédic, and D. Louër, *Solid State Ionics,* in press.
6. S. Westman, P.-E. Werner, T. Schuler, and W. Raldow, *Acta Chem. Scand. A* **35,** 467 (1981).
7. D. Pelloquin, M. Louër, and D. Louër, *J. Solid State Chem.* **112,** 182 (1994).
8. M. Boll, "Memento du Chimiste." Dunod, Paris (1949).
9. D. Louër and J. I. Langford, *J. Appl. Crystallogr.* **21,** 430 (1988).
10. D. Louër, *Mater. Sci. Forum* **79–82,** 17 (1991).
11. J. Rodriguez Carvajal, *In* "Collected Abstracts of Powder Diffraction Meeting," p. 127. Toulouse, France, 1990.
12. G. M. Sheldrick, *Acta Crystallogr. A* **46,** 467 (1990).
13. G. M. Sheldrick, "SHELXL93, Program for the Refinement of Crystal Structures." Univ. of Göttingen, Germany.
14. M. Louër and D. Louër, *Adv. X-ray Anal.* **37,** 21 (1994).
15. D. Louër and M. Louër, *J. Appl. Crystallogr.* **5,** 271 (1972).
16. A. Boultif and D. Louër, *J. Appl. Crystallogr.* **24,** 987 (1991).
17. A. D. Mighell, C. R. Hubbard, and J. K. Stalick, "A FORTRAN Program for Crystallographic Data Evaluation," Nat. Bur. Stand. (U.S.) Tech. Note 1141, 1981. [NBS*AIDS83 is an expanded version of NBS*AIDS80]
18. International Centre for Diffraction Data, NIST CDF database, Newtown Square, PA.
19. International Centre for Diffraction Data, Newtown Square, PA.
20. N. Miliinski, P. Radivojevic, and B. Ribár, *Cryst. Struct. Comm.* **11,** 1241 (1982).
21. A. Leclaire, *J. Solid State Chem.* **28,** 235 (1979).